

CONSTRAINTS ON Ω_m , Ω_Λ , AND σ_8 FROM COUNTS OF GALAXY CLUSTERSGILBERT HOLDER¹, ZOLTÁN HAIMAN^{2,3}, JOSEPH MOHR⁴¹ Department of Astronomy and Astrophysics, University of Chicago, Chicago IL 60637² Princeton University Observatory, Princeton NJ 08544⁴ Departments of Astronomy and Physics, University of Illinois, Urbana IL 61801
holder@oddjob.uchicago.edu, haiman@astro.princeton.edu, mohr@rockie.uchicago.edu*Draft version December 2, 2024*

ABSTRACT

We show that the counts of galaxy clusters in future deep cluster surveys can place strong constraints on the matter density, Ω_m , the vacuum energy density, Ω_Λ , and the normalization of the matter power spectrum, σ_8 . Degeneracies between these parameters are different from those in studies of either high-redshift type Ia Supernovae (SNe), or cosmic microwave background (CMB) anisotropies. This complementarity will allow joint constraints on parameters with improved accuracy. Using a mass threshold for cluster detection expected to be typical for upcoming SZE surveys, we find that constraints on Ω_m and σ_8 at the level of roughly 5% or better can be expected, assuming redshift information is known at least to $z \sim 0.5$. Without information past this redshift, Ω_Λ is constrained to 25%. With complete redshift information, deep ($M_{\text{lim}} \sim 10^{14} h^{-1} M_\odot$), relatively narrow ($\sim 12 \text{deg}^2$) surveys, can further constrain Ω_Λ to an accuracy of $\sim 15\%$, while large-area surveys such as PLANCK or large ground-based bolometer arrays could measure Ω_Λ to a precision of $\sim 4\%$ or better.

Subject headings: cosmic microwave background — cosmology: theory — large-scale structure of universe — cosmological parameters

1. INTRODUCTION

The abundance of galaxy clusters can provide strong constraints on cosmological parameters (e.g., Bahcall and Fan 1998; Viana and Liddle 1999). Future cluster surveys, especially using the Sunyaev-Zeldovich effect, will provide large catalogs of clusters with a selection function which is remarkably unbiased (Barbosa *et al.* 1996; Holder *et al.* 2000; Kneissl *et al.* 2001). Cluster surveys probe the amplitude of the power spectrum as a function of redshift and the cosmic volume per unit redshift and solid angle (Haiman, Mohr and Holder 2000, hereafter HMH). This allows unique constraints on cosmology, and provides a sensitive test of structure formation. As we show below, cluster counts out to $z \sim 0.5$ are powerful probes of Ω_m and σ_8 , while a deeper cluster inventory will allow a determination of the vacuum energy density, Ω_Λ , as well.

In HMH we showed expected constraints on the equation of state of the dark energy and the matter density, assuming a flat universe and two specific proposed cluster survey instruments. In this work, we specialize to the case of vacuum energy (equation of state $w \equiv dp/d\rho = -1$), but generalize to non-flat universes; we also use the normalization of the matter power spectrum σ_8 as a free parameter. Here we use less realistic mass limits for cluster detection, to focus on the effects of abundance evolution and volume as opposed to the particulars of the instruments. Interpreting a future cluster survey will require careful consideration of the survey selection function.

In § 2, we outline our methods for calculating survey yields, while § 3 outlines our statistical methods. In § 4, we present our results and conclude with a discussion of possible systematic errors and future work that will be necessary to achieve the expected constraints.

³ Hubble Fellow

2. CALCULATING CLUSTER SURVEY YIELDS

To calculate the expected number of clusters per square degree as a function of redshift one must consider several elements: the comoving volume per unit redshift and unit solid angle, $dV/dzd\Omega$, the minimum observable mass as a function of redshift and cosmology, $M_{\text{lim}}(z)$, and the comoving number density of halos above the mass threshold as a function of redshift and cosmology, $n(> M_{\text{lim}}, z)$.

The comoving volume per unit redshift is straightforward to calculate (e.g., Peebles 1993), and for this work we assume that the mass threshold is constant with redshift and cosmology, approximately consistent with expectations for surveys using the Sunyaev-Zeldovich effect (Holder *et al.* 2000; Bartlett 2000; Kneissl *et al.* 2001). The mass threshold of detectability in a survey is very important, and it is likely that such a mass threshold will have a dependence on cosmology. We ignore the cosmological dependence in this work in order to isolate the effect of the growth rate of structure as a function of cosmology as the primary discriminant between cosmological models. We note that mass limits are generally sensitive to the cluster baryon fraction, so that in a more realistic study, the mass limit should be taken to be a function of Ω_B and Ω_m . Furthermore, for an X-ray survey, the dependence of the mass limit on cosmology can be the dominant effect (more important than the growth function) that drives the differences in cluster abundance among cosmologies (see HMH, who also find that in comparison, changes in the growth function are the most important effect in an SZE survey).

For the comoving number density of clusters, we use the mass function of dark matter halos obtained from large cosmological simulations (Jenkins *et al.* 2000), where the comoving number density of clusters between mass M and

$M + dM$ is given by

$$\frac{dn}{dm} = 0.315 \frac{\rho_o}{M^2} \frac{d \ln \sigma^{-1}}{d \ln M} \exp[-|\ln \sigma^{-1} + 0.61|^{3.8}] \quad , \quad (1)$$

where $\sigma(M, z)$ is the variance in the density field smoothed on a scale corresponding to mass M and ρ_o is the present-day mean density of the universe.

From linear theory, $\sigma(M, z)$ can be separated into $\sigma(M, z) = \sigma(M, z = 0)D(z)$, where $D(z)$ is the linear growth factor. We calculate $D(z)$ directly from linear theory (e.g., Peebles 1993). The variance $\sigma(M, z = 0)$ is calculated with a top hat filter of radius appropriate for mass M , using the matter power spectrum calculated from the fitting functions of Eisenstein and Hu (1999).

As a fiducial model, we take a flat, low-density model, with $\Omega_m = 0.3$, $\Omega_\Lambda = 0.7$, $h = 0.65$, $\sigma_8 = 1.0$, $n = 1$, and $\Omega_b h^2 = 0.02$. We keep h , n and $\Omega_b h^2$ fixed for all models and vary the remaining three parameters. To isolate the effects of the growth of the power spectrum, we artificially constrain the power spectrum to be that of the fiducial model for all models. In the absence of modifications to the power spectrum, these results are absolutely unchanged by varying h or $\Omega_b h^2$. Relaxing the assumption of a fixed power spectrum will slightly affect the constraints on parameters, but the qualitative results are unchanged, as the shape of the power spectrum has only a mild effect on the cluster abundance (there would be no dependence on the power spectrum if it was a pure power law, see HMH). Large scale structure measurements, from the spatial distribution of either galaxies or galaxy clusters should be able to provide accurate measurements of the matter power spectrum over the range of interest.

3. ESTIMATING CONSTRAINTS ON COSMOLOGY

To estimate constraints on cosmological parameters, we assume Poisson errors on finely binned ($\Delta z = 0.01$) model predictions. Still finer binning was found to not affect the results. We determine confidence regions in two ways, using a Monte Carlo method and the Fisher matrix (Eisenstein, Hu, and Tegmark 1999).

In the first method, we construct a likelihood space by a Monte Carlo method, generating 3000 realizations of the input fiducial model, in the form of mock catalogs of clusters at different redshifts, and then fitting each realization, allowing Ω_m , Ω_Λ and σ_8 to find their best-fit values. In this way, we can map out regions of parameter space that contain 68% and 95% of the realizations.

For the case of Gaussian errors, the likelihood is simply related to the usual χ^2 statistic as $-2 \ln \mathcal{L} = \chi^2$. In the case of Poisson errors, it can be shown that the analogous statistic is the Cash C statistic (Cash 1979):

$$-2 \ln \mathcal{L} = -2 \sum_{a=1}^N n_a \ln e_a - e_a - \ln n_a! \quad , \quad (2)$$

where n_a and e_a are the observed and expected number of counts in bin a , respectively, and N is the total number of bins.

A computationally more efficient method to estimate confidence regions is to use the Fisher matrix. We constructed the second derivatives of the log likelihood with respect to the parameters of interest at the position in

likelihood space of the fiducial model. Ensemble averaging then leads to a simple expression for the Fisher matrix:

$$\frac{-\partial^2 \ln \mathcal{L}}{\partial p_i \partial p_j} = \sum_{a=1}^N \frac{\partial e_a}{\partial p_i} \frac{\partial e_a}{\partial p_j} \frac{1}{m_a} \quad , \quad (3)$$

where m_a is the number expected in the fiducial model in bin a and the p_i are the parameters of interest, in this case Ω_m , Ω_Λ , and σ_8 . This is also what one would obtain assuming a Gaussian probability distribution with $\sigma^2 = N$ and using the usual χ^2 estimator for the likelihood.

Assuming that the likelihood distribution is approximately Gaussian near the peak likelihood, we can use confidence limits for Gaussian statistics (i.e., χ^2) to obtain 68% and 95% confidence regions.

The advantage of the Fisher matrix method is that it is very fast and gives accurate results if the likelihood space is well-behaved. While we have no reason to suspect this is not the case, we perform the Monte Carlo analysis as a useful check. The Fisher matrix approximates confidence regions as Gaussian ellipsoids, while the true confidence regions could have broad tails or significant curvature.

4. RESULTS

We first look at a relatively low value for the constant mass limit, $M_{\text{lim}} = 10^{14} h^{-1} M_\odot$, appropriate for a deep SZE survey that would cover approximately 12 deg². In Figure 1, we show the expected number of clusters as a function of redshift, as well as the likelihood contours we find in three different projections in the Ω_m , Ω_Λ , σ_8 plane. The figure reveals that the constraints from the Monte Carlo method are similar to those obtained from the Fisher matrix method, especially in the Ω_m - Ω_Λ plane. This indicates that the likelihood space is well-behaved, with degeneracies manifesting themselves as ellipses. As the Fisher matrix method is much faster, this allows a much more extensive study of parameters. However, the differences are not negligible for the plots involving σ_8 , suggesting that the likelihood space in the σ_8 direction is significantly non-Gaussian.

Constraints on Ω_m and Ω_Λ from cluster surveys are complementary to other probes. Figure 1 also shows the current constraints on parameters from studies of distant supernovae, as well as the $\Omega_m + \Omega_\Lambda = 1$ line expected from inflation and preferred by CMB studies (de Bernardis *et al.* 2000; Hanany *et al.* 2000; Netterfield *et al.* 2001; Pryke *et al.* 2001). The different orientations of the parameter degeneracies suggest that joint constraints from CMB measurements, supernovae, and deep cluster surveys will be a powerful probe of both cosmological parameters and potential systematic effects in other data sets. In addition, Figure 1 shows that the degeneracy in the Ω_m - σ_8 plane is in a different direction when compared with local determinations from massive ($M \gtrsim 2 \times 10^{15} h^{-1} M_\odot$) clusters (Viana and Liddle 1999). This is due to the different mass and redshift ranges probed, with the current local determinations coming from much more massive clusters (HMH).

When marginalized over the other two parameters, we can expect uncertainties in Ω_m , Ω_Λ , and σ_8 of 6%, 15%, and 3%, respectively, assuming complete redshift information. The relatively small number of (~ 400) clusters spread over only a few square degrees should allow follow up observations to get redshift information.

Large ground-based telescopes equipped with bolometer arrays will be efficient at detecting clusters through their SZ effect. We assume a typical mass limit for such instruments to be $2.5 \times 10^{14} h^{-1} M_{\odot}$ and a typical sky coverage of 4000 deg². We again calculate constraints on cosmological parameters using the Fisher matrix, with results shown in Figure 2. In this case, the possible constraints on cosmology are approximately an order of magnitude stronger than the first case. The direction of the degeneracy is slightly different from Figure 1, due to the different redshift distribution and mass range. This indicates the potential power of using the distribution of observed clusters in mass, which we have not utilized in this paper, but will explore in future work. The offset between the local Ω_m - σ_8 determination and our central value is an artifact of our assumed fiducial model being slightly offset from the best fit of Viana and Liddle (1999), although our fiducial model is well within their quoted uncertainties.

Single parameter uncertainties on Ω_m , Ω_{Λ} , and σ_8 are expected to be approximately 0.7%, 2%, and 0.5% respectively, for this case, assuming complete redshift information. Again, redshift information will be very important for such tests. In this case, redshifts for clusters spread over 4000 deg² is a non-trivial task, but it is clear from Figure 2 that the reward for such an exercise will be precise measurements of cosmological parameters.

We finally adopt a relatively high value for the limiting mass, $M_{\text{lim}} = 8 \times 10^{14} h^{-1} M_{\odot}$, appropriate for an SZE survey like PLANCK, covering a large fraction of the sky (we assume 50%). From Figure 3, it can be seen that such a survey will allow strong constraints on cosmological parameters, comparable to those expected from the second case above. Even with only ~ 1 cluster per square degree, the large survey area allows a large catalog to be assembled.

In this case, full-sky coverage of redshifts is clearly going to be difficult. A reasonable strategy would be to cross-correlate with a large area survey such as the SDSS. For example, it could be reasonably expected that every cluster found by PLANCK with $z < 0.5$ will appear in the SDSS catalog in regions of overlapping coverage. Using only those clusters with $z < 0.5$, and again assuming 50% of the sky is covered (although SDSS will only cover $\sim 25\%$), Figure 3 shows the expected constraints on parameters. The constraints on σ_8 and Ω_m are still strong, but with only the nearby sample it is difficult to constrain the vacuum energy. The growth function is not very sensitive to vacuum energy out to this redshift, and therefore there is little difference in the comoving number density as a function of vacuum energy density. It is the information from clusters past $z \sim 0.5$ that carry almost all constraints on the cosmological constant. This is unfortunate, as these will be the clusters that will be most difficult to follow up. For smaller surveys, deep imaging of a fairly small region of the sky will be reasonably straightforward. However, the sparse sampling of the very distant clusters in the PLANCK sample will make targeted follow-up difficult.

Single parameter uncertainties on Ω_m , Ω_{Λ} and σ_8 , assuming complete redshift information are 1%, 4%, and 0.9%, respectively for a survey like PLANCK. For redshift information only out to $z = 0.5$, these numbers become

2%, 26%, and 2%, respectively. Since the $z < 0.5$ sample is roughly half the size of the full sample, the changes in Ω_m and σ_8 are barely larger than would be expected from the Poisson error of \sqrt{N} in the total number of clusters. For a ground-based bolometer array, the same effect can be observed, with expected uncertainties of 3%, 23%, and 3%, respectively, without redshift information past $z = 0.5$.

5. CONCLUSIONS AND FUTURE WORK

We have shown that cluster surveys have the potential to be powerful probes of cosmological parameters, and in a manner that will serve as a useful check of other methods. Efficient follow-up to obtain redshift information will be crucial, with most information on Ω_{Λ} coming from clusters with $z > 0.5$. This argument would favor a deep survey on a relatively small patch of sky, as follow-up observations could be done on a smaller scale.

The results obtained here are based on highly idealized toy models, and are far from realistic in several respects. Most importantly, we have not addressed here the effects of systematic errors from cluster evolution, which can mimic different values of cosmological parameters (but see HMH for a quantitative discussion). In addition, although we expect the matter power spectrum to cause relatively little cosmological sensitivity (from HMH), this deserves further study (note that we can expect accurate measurements of the shape of the matter power spectrum on the scales of interest in the near future from galaxy surveys such as SDSS and 2DF). We assume that Poisson errors are setting the uncertainty on cosmological parameters. With surveys in the design stage, it is difficult to estimate the potential systematic errors that will be important in any interpretation of real surveys.

We have only looked at the redshift evolution of cluster counts, and not used the mass function at each redshift as a further constraint on cosmology. The mass function, in principle, carries a significant amount of information on cosmology and could also be a source of systematic error in an interpretation of survey results. The mass function has been accurately (to an overall error of 30 percent) determined in a handful of cosmologies by Jenkins et al. (2000). It will be important to repeat similar numerical experiments in a broader range of cosmologies, to have a better understanding of the scaling of the mass function with cosmology.

Mass limits as a function of cosmology must be well-understood to interpret the source counts. This includes both evolution with redshift and scatter in the “detectability” at a given mass. Although temperatures can be obtained for clusters in a cosmologically independent way from their X-ray spectra, the relation of this temperature to the halo mass in different cosmologies needs further study. Extracting unbiased cosmological parameters from real survey data will require multi-wavelength follow-up of at least a sub-sample of the detected clusters.

Just as large scale structure surveys have learned about galaxy evolution and CMB experiments have learned about foregrounds, cluster surveys will learn about galaxy cluster structure and evolution. As the largest virialized objects in the universe, clusters at high redshift will yield a wealth of information on galaxy formation and other aspects of cosmology. A study of cluster scaling relations

that combines SZE and X-ray data can help in separating the systematic effects arising from the assumption of virialization from cosmology (Verde, Haiman and Spergel, in preparation).

None of these issues should, in principle, prevent robust and highly precise constraints on cosmological parameters from cluster surveys. The justified use of the Fisher matrix will enable fast exploration of many cosmological parameters. The small subset explored here and in HMH suggest that these constraints should be highly complementary to large scale structure studies (e.g., Phillips et al. 2000), CMB anisotropies, and probes of distance, such as type Ia supernovae. In addition, tracing the redshift evolution of the cluster abundance offers a unique opportunity to track the growth of structure that is expected from hierarchical

clustering, providing a strong test of the underlying cold dark matter model.

We acknowledge many useful discussions with John Carlstrom, Michael Turner and David Spergel. GPH was supported in part by a DOE grant to the University of Chicago. ZH is supported by NASA through the Hubble Fellowship grant HF-01119.01-99A, awarded by the Space Telescope Science Institute, which is operated by the Association of Universities for Research in Astronomy, Inc., for NASA under contract NAS 5-26555. JMM is supported in part by grants G01-2125X and AR1-2002X awarded by the Chandra Science Center. The Chandra Science Center is operated by the Smithsonian Astrophysical Observatory for NASA under contract NAS8-39073.

REFERENCES

Bahcall, N. and Fan, X. 1998, *Ap. J.*, **504**, 1.
 Barbosa, D., Bartlett, J., Blanchard, A., and Oukbir, J. 1996, *A&A*, **314**, 13.
 Bartlett, J. G. 2000, *A&A*, submitted.
 Cash, W. 1979, *Ap. J.*, **228**, 939–947.
 de Bernardis, P. et al. 2000, *Nature*, **404**, 955.
 Eisenstein, D. J. and Hu, W. 1999, *Ap. J.*, **511**, 5.
 Eisenstein, D. J., Hu, W., and Tegmark, M. 1999, *Ap. J.*, **518**, 2.
 Haiman, Z., Mohr, J. J., and Holder, G. P. 2000, *Ap. J.*, in press: astro-ph/0002336.
 Hanany, S. et al. 2000, *ApJ*, submitted. astro-ph/0005123.
 Holder, G. P., Mohr, J. J., Carlstrom, J. E., E., E. A., and Leitch, E. M. 2000, *Ap. J.*, **544**, 629.
 Jenkins, A., Frenk, C. S., White, S. D. M., Colberg, J. M., Cole, S., Evrard, A. E., Couchman, H. M. P., and Yoshida, N. 2001, *Mon. Not. Roy. Ast. Soc.*, **321**, 372+.
 Kneissl, R., Jones, M. E., Saunders, R., Eke, V. R., Lasenby, A. N., Grainge, K., and Cotter, G. 2001, submitted: *Mon. Not. Roy. Ast. Soc.*, astro-ph/0103042.
 Netterfield, C. B. et al. 2001, *Ap. J.*, submitted, astro-ph/0104460.
 Peebles, P. 1993. *Principles of Physical Cosmology*. Princeton University Press, Princeton.
 Phillips, J., Weinberg, D. H., Croft, R. A. C., Hernquist, L., Katz, N., and Pettini, M. 2000, *Ap. J.*, submitted, astro-ph/0001089.
 Pryke, C., Halverson, N. W., Leitch, E. M., Kovac, J., Carlstrom, J. E., Holzapfel, W. L., and Dragovan, M. 2001, *Ap. J.*, submitted, astro-ph/0104490.
 Viana, P. and Liddle, A. 1999, *Mon. Not. Roy. Ast. Soc.*, **303**, 535.

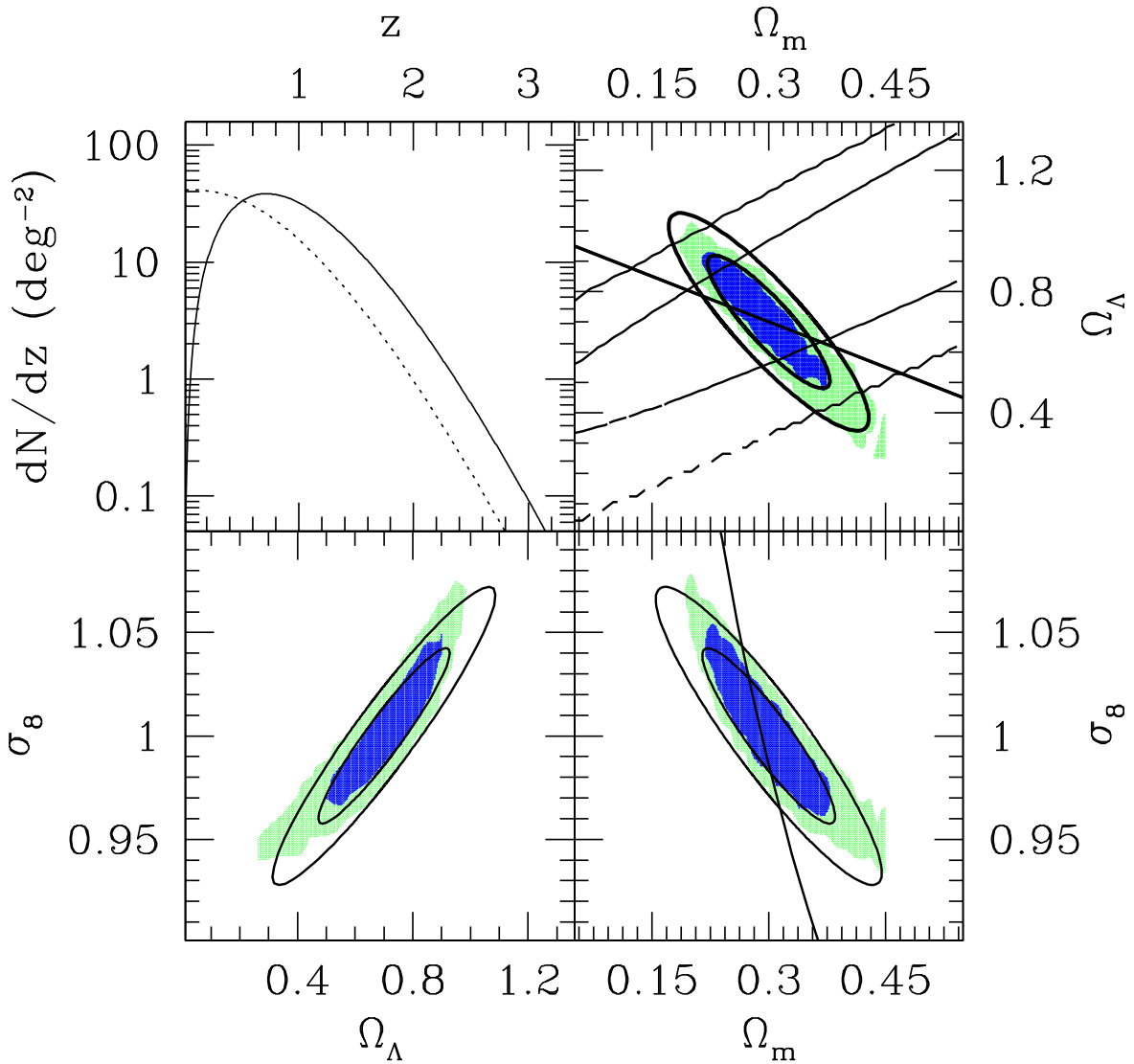


FIG. 1.— Top left panel: differential (solid curve) and cumulative (dashed curve) number counts of clusters as a function of redshift. A mass limit of $10^{14} h^{-1} M_\odot$ is assumed. Top right panel: 68% and 95% confidence levels on Ω_m - Ω_Λ marginalized over σ_8 . Shaded regions are from a Monte Carlo analysis, while contours show results using the Fisher matrix. Dashed contours show the current constraints from the Supernova Cosmology Project (see <http://supernova.lbl.gov>), while the diagonal solid line indicates a flat universe favored by CMB anisotropies. Bottom right panel: Confidence levels on Ω_m - σ_8 marginalized over Ω_m , similar to the top right panel. The diagonal line shows the degeneracy from the abundance of massive ($M \gtrsim 2 \times 10^{15} M_\odot$) local clusters. Bottom left panel: Confidence levels on Ω_Λ - σ_8 (bottom right), marginalized over Ω_m .

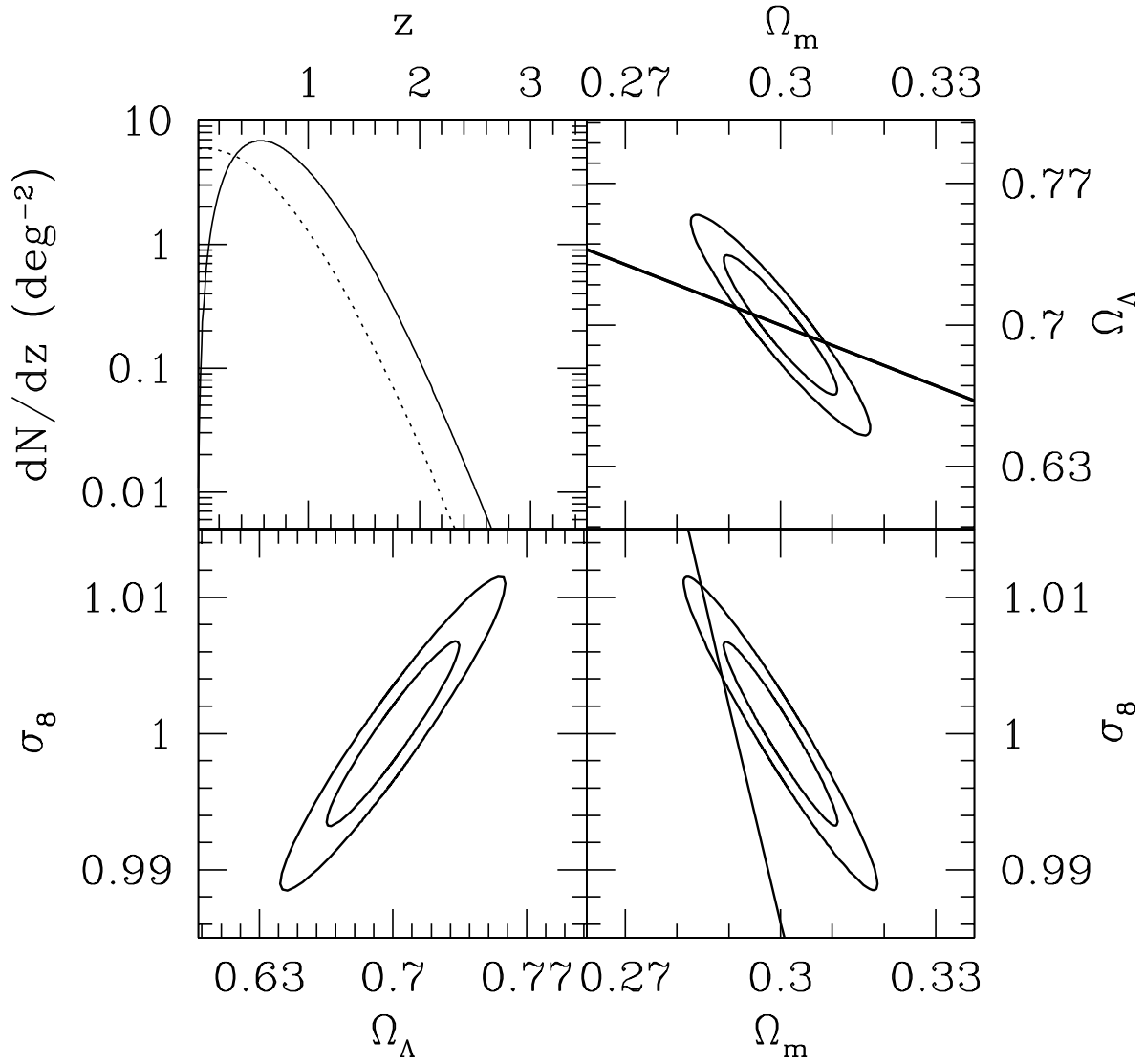


FIG. 2.— Confidence levels on parameters, marginalized over the third parameter in the likelihood space, as in Figure 1, but for a higher mass limit of $2.5 \times 10^{14} h^{-1} M_{\odot}$. Contours show the expected 68% and 95% confidence regions, using the Fisher matrix. Relative axis scaling and the labeling of the curves is the same as Figure 1, except in the upper right panel, where we have omitted showing the constraints from SNe.

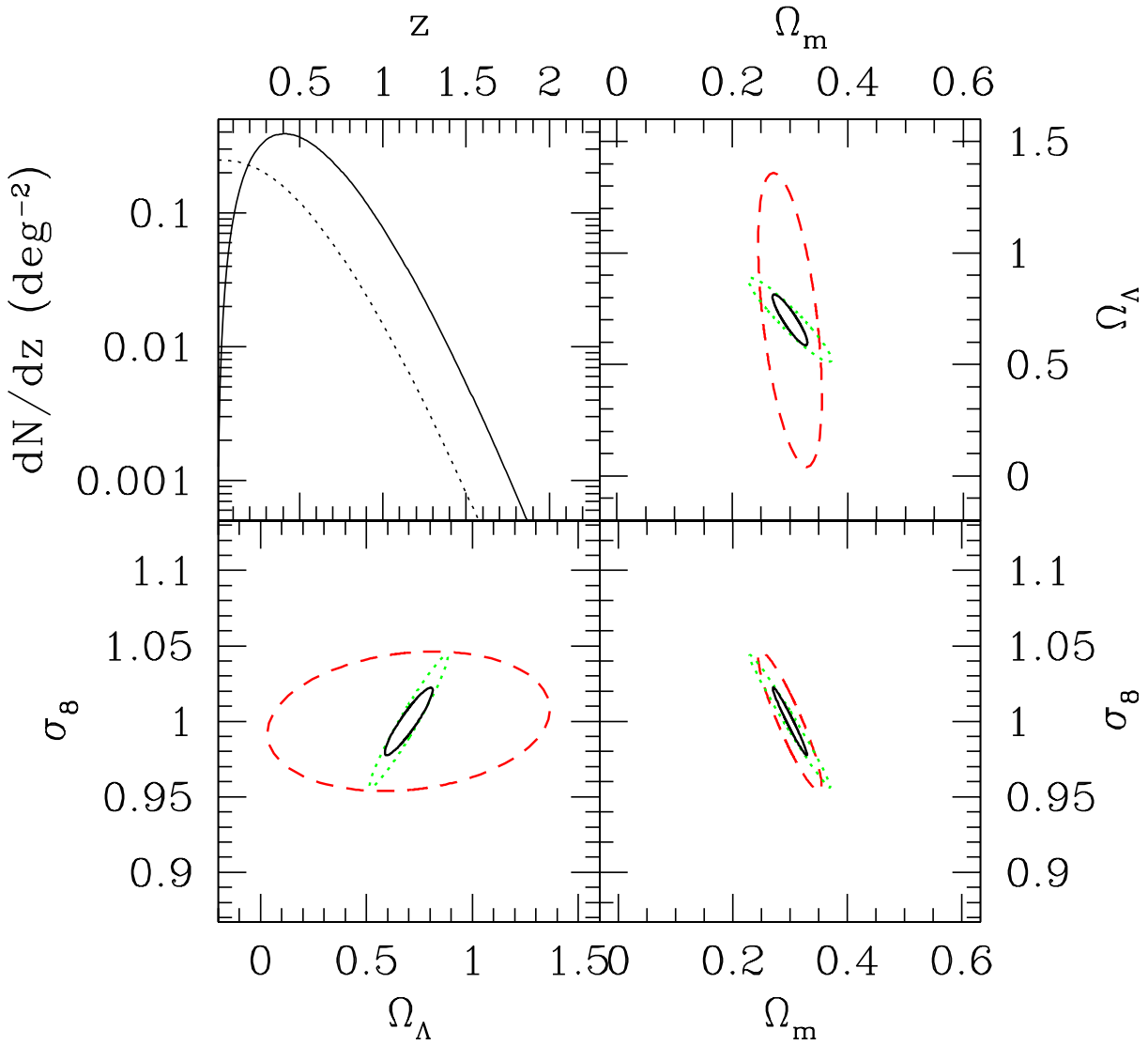


FIG. 3.— Confidence levels on parameters, using the Fisher matrix as in Figure 2, but for a mass limit of $8 \times 10^{14} h^{-1} M_\odot$. Dashed ellipses show the expected 95% confidence regions using only clusters with $z < 0.5$, dotted curves show the 95% confidence regions using only clusters with $z > 0.5$, while solid curves show the 95% confidence region for the entire sample. Relative axis scaling is the same as Figure 1.